Functional Templates in fMRI: Building Accurate and Interpretable Group-Level Decoders

Pierre-Louis Barbarant (pierre-louis.barbarant@inria.fr)
Université Paris-Saclay, Inria, CEA, Palaiseau 91120, France
Cognitive Neuroimaging Unit, NeuroSpin (INSERM-CEA), University of Paris-Saclay, Gif-sur-Yvette, France
GHU Paris, psychiatrie et neurosciences, Hôpital Saint-Anne, institut de neuromodulation, Paris, France

Florent Meyniel (florent.meyniel@cea.fr)
Cognitive Neuroimaging Unit, NeuroSpin (INSERM-CEA), University of Paris-Saclay, Gif-sur-Yvette, France
GHU Paris, psychiatrie et neurosciences, Hôpital Saint-Anne, institut de neuromodulation, Paris, France

Bertrand Thirion (bertrand.thirion@inria.fr)
Université Paris-Saclay, Inria, CEA, Palaiseau 91120, France

Abstract

Anatomical and functional inter-individual variability poses a significant challenge to group analyzes in neuroimaging studies. While anatomical templates help to mitigate morphological differences by coregistering subjects in fMRI, they fail to account for functional variability, often leading to blurred activation patterns on the template due to group-level averaging. To address this, hyperalignment identifies fine-grained correspondences between functional brain maps of different subjects, with Procrustes analysis and Optimal Transport being among the most effective approaches. However many hyperalignment-based imaging studies rely on selecting a single target subject as the reference to which all other subjects' data are aligned. We argue that a functional template obviates the need for this arbitrary selection, effectively encapsulating population similarities while preserving anatomical coherence. Using several tasks from the Individual Brain Charting dataset, we assess the benefit of hyperalignment on template estimation and on decoding accuracy. Our results show that (a) functional templates produce more localized activation clusters than traditional anatomical averaging, improving the interpretability of population-level studies, and (b) they preserve or enhance the semantic content of brain activations, leading to comparable or higher classification accuracies in most tasks compared to anatomical or pairwise functional alignment.

Keywords: fMRI; Functional Alignment; Brain Decoding

Introduction

In functional magnetic resonance imaging (fMRI), comparing neural activity patterns across individuals presents a fundamental challenge due to variations in both brain anatomy and function. Traditional anatomical normalization approaches map individual brains onto standard templates (Fonov et al. (2009)), but do not adequately capture functional differences between subjects (Haxby et al. (2001); Sabuncu et al. (2009)).

Functional alignment has emerged as a complementary approach, with current techniques falling into two categories: pairwise and template-based approaches. Pairwise methods, including Procrustes Analysis (Guntupalli et al. (2016)) and Optimal Transport (OT)-based alignment (Bazeille et al. (2019)), directly map functional responses between pairs of subjects but introduce potential bias through reference subject selection.

Template-based functional alignment addresses these limitations by creating a shared representational space. Methods such as Hyperalignment (Guntupalli et al. (2016)) and Wasserstein barycenters (Agueh & Carlier (2011)) eliminate arbitrary subject selection and have shown promise in improving group-level analyses (Jeganathan et al. (2024)). Unlike the Shared Response Model (SRM) (Chen et al. (2015)) which relies on latent space representation, functional templates in image space maintain direct correspondence with brain anatomy, providing interpretable composite representations.

Our study addresses key knowledge gaps by conducting a comprehensive evaluation using the Individual Brain Charting (IBC) dataset (Pinho et al. (2018)). We compare pairwise versus template-based alignment methods and examine their impact on task decoding performance, specifically evaluating Procrustes and Optimal Transport approaches in both contexts.

Methods

Alignment Methods

We evaluate two alignment approaches in both pairwise and template-based configurations:

Procrustes Analysis seeks an orthogonal transformation matrix $\mathbf{M}$ and scaling factor s that optimally align source and target task maps by minimizing:

$$\min_{\mathbf{P}=s\mathbf{M}} \|\mathbf{F}^s\mathbf{P} - \mathbf{F}^t\|_F^2 \tag{1}$$

Optimal Transport computes a transport plan $\mathbf{P}$ that minimizes the cost of mapping voxel-wise responses with entropic regularization:

$$\min_{\mathbf{P}} \mathrm{Tr}(\mathbf{PC}) + \varepsilon\mathbf{E}(\mathbf{P}) \tag{2}$$

For computational tractability and to constrain voxel correspondences within anatomically meaningful neighborhoods (avoiding spurious long-range correspondences), we adopt a piecewise alignment approach using the Schaefer atlas with 400 parcels (Schaefer et al. (2017)) following Bazeille et al. (2021).

Template Construction follows an alternating minimization scheme where the template $\mathbf{F}^T$ minimizes:

$$\mathbf{F}^T \in \arg\min_{\mathbf{F}} \sum_{s=1}^{S} \|\mathbf{F}^s\mathbf{P}^s - \mathbf{F}\|_F^2 \tag{3}$$

Dataset and Evaluation

We used fMRI data from the Individual Brain Charting (IBC) dataset comprising 13 participants across six tasks: Audio, FaceBody, Mario, MathLanguage, RSVPLanguage, and Working Memory. Data were preprocessed using Pypreprocess with anatomical registration to the 3mm MNI152NLin2009cAsym template.

Task-based decoding analysis employed leave-one-subject-out cross-validation. For pairwise alignments, training data from all subjects except the test subject were projected onto the test subject's space. For template-based alignments, a functional template was constructed and all subjects' data projected onto this common space. We used `fmralign`[1] for functional alignment and linear support vector classifiers for classification.

[1] `https://github.com/Parietal-INRIA/fmralign`

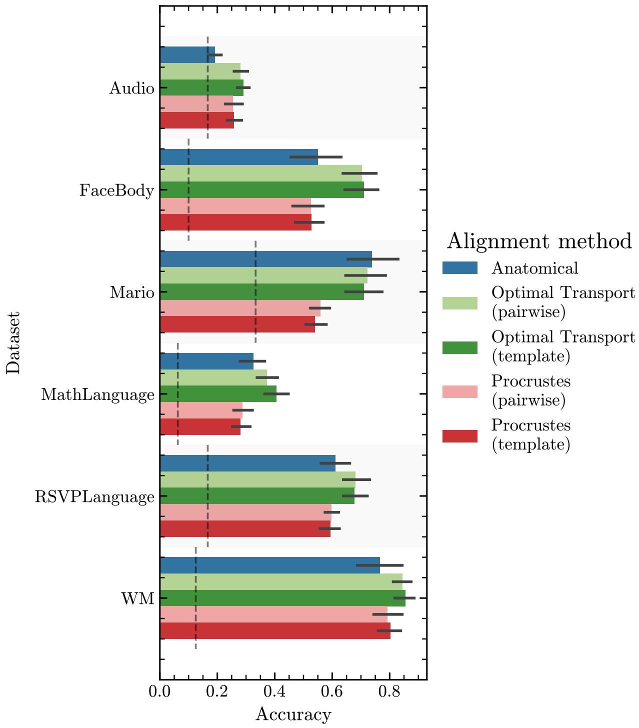

Figure 1: **Task classification accuracies across alignment methods.** Classification accuracies using leave-one-subject-out cross-validation, with one accuracy score per subject. Error bars denote variance across subjects. Anatomical alignment provides baseline performance using only anatomical template registration. Template-based methods align all subjects to a common functional template before cross-validation. Pairwise methods align training subjects to the left-out test subject. Dashed lines indicate chance-level performance.

Results

Figure 1 presents task classification results across alignment methods. Template-based Optimal Transport (OT) achieved the highest classification accuracy on 5/6 tasks, with anatomical alignment performing best only on the Mario task. OT-based approaches consistently outperform Procrustes methods across all tasks, with template-based OT being the only method to systematically exceed the anatomical baseline. Statistical significance testing confirms these performance differences, with OT methods showing significant improvements ($p < 0.01$ to $p < 0.001$) over anatomical alignment on most tasks. Besides improved decoding accuracy, functional template alignment also affects the spatial organization of task-discriminatory brain regions. Figure 2 demonstrates this effect by analyzing the distribution of cluster sizes for discriminatory voxels. While anatomical alignment produces broadly distributed activation patterns, template alignment methods generate more spatially concentrated clusters of both activation t-values and weights, while maintaining similar voxel-wise distribution profiles for both measures.

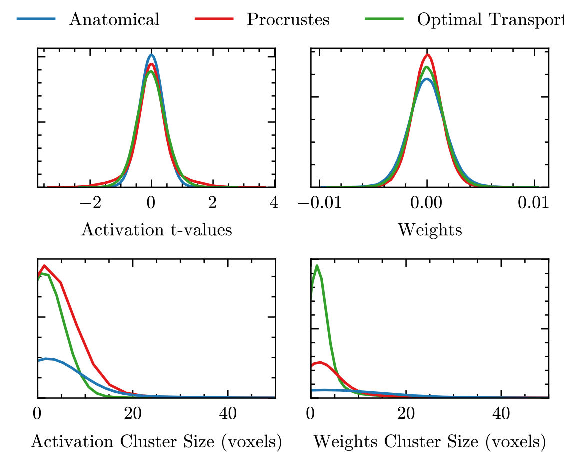

Figure 2: **Distributions of t-values and weights after template alignment.** Top row displays the distribution profiles of t-values and classifier weights across different template-based methods, illustrating how alignment techniques influence statistical parameter distributions for the FaceBody task. Bottom row quantifies the distribution of cluster sizes across methods for both activation patterns and decoder weights. Clusters were defined as connected components after thresholding at the top 20% of each quantity of interest.

Discussion

Our findings confirm the advantage of template-based alignment over pairwise methods in functional alignment, with OT-based template alignment achieving the highest overall classification accuracy. This approach offers three key benefits:

Computational Efficiency – Template-based alignment requires only S projections (one per subject) compared to $S(S-1)$ projections for pairwise methods in cross-validation scenarios, significantly reducing computational cost.

Enhanced Interpretability – Unlike latent-space methods such as SRM, functional templates maintain direct correspondence with brain anatomy, allowing traditional neuroimaging analysis while creating more spatially focused activation and classification patterns compared to anatomical registration.

Superior Performance – Template-based OT alignment achieves superior decoding performance while simultaneously simplifying the alignment process by eliminating the need to select a reference subject. This removal of arbitrary reference subject selection not only reduces methodological bias but also leads to enhanced classification accuracy, demonstrating that the template-based approach provides both methodological and performance advantages over pairwise alignment methods.

Acknowledgments

This work has benefited from State support as part of the Audace! Programme led by the CEA and managed by the Agence Nationale de la Recherche under the France 2030 heading, bearing the reference “ANR24-RRII-0004”.

References

Agueh, M., & Carlier, G. (2011, January). Barycenters in the wasserstein space. *SIAM Journal on Mathematical Analysis*, *43*(2), 904–924. doi: 10.1137/100805741

Bazeille, T., DuPre, E., Richard, H., Poline, J.-B., & Thirion, B. (2021, December). An empirical evaluation of functional alignment using inter-subject decoding. *NeuroImage*, *245*, 118683. doi: 10.1016/j.neuroimage.2021.118683

Bazeille, T., Richard, H., Janati, H., & Thirion, B. (2019). Local optimal transport for functional brain template estimation. In *Lecture notes in computer science* (pp. 237–248). Springer International Publishing. doi: 10.1007/978-3-030-20351-1_18

Chen, P.-H. C., Chen, J., Yeshurun, Y., Hasson, U., Haxby, J., & Ramadge, P. J. (2015). A reduced-dimension fmri shared response model. In C. Cortes, N. Lawrence, D. Lee, M. Sugiyama, & R. Garnett (Eds.), *Advances in neural information processing systems* (Vol. 28). Curran Associates, Inc.

Fonov, V., Evans, A., McKinstry, R., Almli, C., & Collins, D. (2009, July). Unbiased nonlinear average age-appropriate brain templates from birth to adulthood. *NeuroImage*, *47*, S102. doi: 10.1016/s1053-8119(09)70884-5

Guntupalli, J. S., Hanke, M., Halchenko, Y. O., Connolly, A. C., Ramadge, P. J., & Haxby, J. V. (2016, March). A model of representational spaces in human cortex. *Cerebral Cortex*, *26*(6), 2919–2934. doi: 10.1093/cercor/bhw068

Haxby, J. V., Gobbini, M. I., Furey, M. L., Ishai, A., Schouten, J. L., & Pietrini, P. (2001, September). Distributed and overlapping representations of faces and objects in ventral temporal cortex. *Science*, *293*(5539), 2425–2430. doi: 10.1126/science.1063736

Jeganathan, J., Paton, B., Koussis, N., & Breakspear, M. (2024). Integrating anatomical and functional landmarks for interparticipant alignment of imaging data. *Imaging Neuroscience*, *2*, 1–16. doi: 10.1162/imag_a_00253

Pinho, A. L., Amadon, A., Ruest, T., Fabre, M., Dohmatob, E., Denghien, I., ... Thirion, B. (2018, June). Individual Brain Charting, a high-resolution fMRI dataset for cognitive mapping. *Scientific Data*, *5*(1), 180105. doi: 10.1038/sdata.2018.105

Sabuncu, M. R., Singer, B. D., Conroy, B., Bryan, R. E., Ramadge, P. J., & Haxby, J. V. (2009, May). Function-based intersubject alignment of human cortical anatomy. *Cerebral Cortex*, *20*(1), 130–140. doi: 10.1093/cercor/bhp085

Schaefer, A., Kong, R., Gordon, E. M., Laumann, T. O., Zuo, X.-N., Holmes, A. J., ... Yeo, B. T. T. (2017, July). Local-global parcellation of the human cerebral cortex from intrinsic functional connectivity mri. *Cerebral Cortex*, *28*(9), 3095–3114. doi: 10.1093/cercor/bhx179